RESEARCH PROGRESS IN MECHANICAL AND MANUFACTURING ENGINEERING VOL. 2 NO. 1
(2021) 117-135
© Universiti Tun Hussein Onn Malaysia Publisher's Office

RPMME

Homepage: http://penerbit.uthm.edu.my/periodicals/index.php/rpmme
e-ISSN : 2773-4765

Interaction of Surface Crack on Solid Shaft Due to Combined Loading

A Syahmi[1], M. K. Awang[1], A. E. Ismail[1], M. N. Ibrahim[1]

[1]Crashworthiness and Collision Research Group (Colored), Faculty of Mechanical and Manufacturing Engineering,
Universiti Tun Hussein Onn Malaysia, Batu Pahat, Johor, MALAYSIA

*Corresponding Author Designation

DOI: https://doi.org/10.30880/rpmme.2021.02.01.014
Received 05 March 2021; Accepted 01 April 2021; Available online 15 April 2021

Abstract:
Fracture is one of the main types of failure in solid cylinders, where the cracks exist when subjected to different types of mechanical loads. These cracks exist in the form of singular or multiple cracks. Multiple cracks can be one of the main reasons that further impacts the failure because the multiple cracks may have an interaction between one another. Therefore, this study is conducted to buckle down the problems that arise from the interactions of multiple cracks subjected to multiple loading. This study focuses on the interaction between multiple cracks located at the surface of the cylinder with parallel and non-coplanar parallel configuration. As the driving force for determining the crack interaction, the stress intensity factor (SIF) is selected. The Ansys finite element program is used to evaluate SIF's different crack geometries and separation distances under various types of mechanical loads. The results show that the effect of crack interaction on parallel cracks and non-coplanar cracks are impacted by shielding and amplifying effect. The angle of inclination between the cracks demonstrates an important role in the interaction because it can change the actions of the interaction from shielding effect to amplifying effects and vice-versa.

Keywords: SIFs, Parallel Cracks, Non-coplanar Parallel Cracks, Single Crack, Interaction Factor, Normalized

1. Introduction

Solid cylindrical shaft has a lot of usage in the modern day. The most prominent use of solid cylindrical shaft in our daily lives is the cylinder head in cars, which is a component in the combustion engine used to close the combustion chamber of the engine top. One of the common reasons for engine breakdown is the cracking of the cylinder head. Therefore, it is important to study the interaction between cracks using fracture mechanics. Fracture mechanics is a form of mechanical study that focuses on the method to predict and diagnose failure due to crack on a member. The main feature of fracture mechanics is to characterise the physical situation near the crack tip in an adequate way, thus providing means for predicting the progress of damage depending on the properties of the material and external

Corresponding author: mdkhair@uthm.edu.my
2021 UTHM Publisher. All right reserved.

load. The presence of a crack in a member magnifies the stress in the surrounding area of the crack and can lead to failure. Cracks act as stress risers and can cause stress in a part to spike near the tip of the crack. The most prominent used to predict crack behaviour is to calculate the 'Stress Intensity Factor'. Stress Intensity Factor, K is a useful concept for characterising the stress field near the crack tip. For this purpose, samples with notches of definite length instead of natural flaws are used. All the different definitions of fracture toughness have in common that they characterise the crack resistance of the material. They can be divided corresponding to the different stages of crack growth: crack initiation, slow crack growth, transition to unstable crack growth, unstable crack growth, and crack arrest.

2. Geometry

2.1 Cylinder geometry

For the proposed condition, which is the parallel cracks on the surface of a solid cylinder is modelled using ANSYS modeller. The dimensions of the shaft will be based on the previous literatures, to ensure that the upcoming results can be verified based on the previous literatures. The diameter for the cylinder will be 50mm and 200mm in length (MK Awang et al, 2017.). The modelled cylinder will then be imported to ANSYS and viewed using ANSYS Mechanical to model the cracks

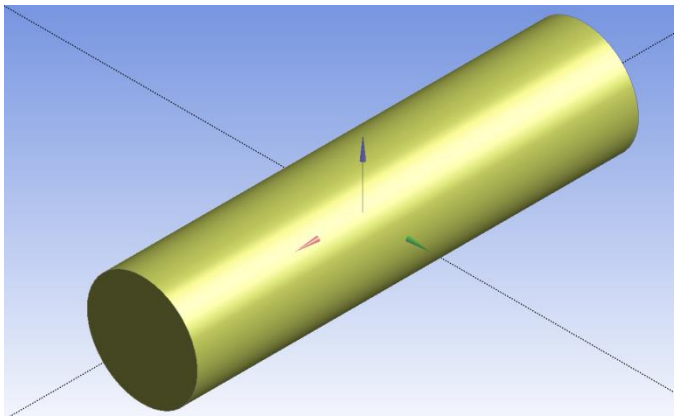

Figure 1: Imported Model of the Specimen in ANSYS Design Modeller

2.2 Crack geometry

The placement of the cracks is be determined using the coordinate systems in ANSYS Mechanical. The Y-axis represents the vertical location of the cracks at the face of the cylinder, while the X-axis represents the horizontal placement of the cracks. The Z axis represents the range between the cracks within the cylinder. The Z-axis of the reference crack will remain unchanged at z=0, while the Z-axis for the observed crack varies with the values of 1, 2, 4, 8, 16, 32 and 64 to represent the c/l values of 0.005, 0.01, 0.02, 0.04, 0.08, 0.16 and 0.32 respectively. The cracks will then be added using the fracture feature with semi elliptical crack shape. Major radius represents the b (horizontal radius) while the minor radius represents the a (vertical radius). These values will be impacted by the values of a/D which ranges from 0.1, 0.2, 0.3, 0.4, while a/b ranges from 0.2 to 1.2 with the increment of 0.2 each (M.K Awang et al, 2017.) to agree with the parameters set by Shin and Chai, 2001.

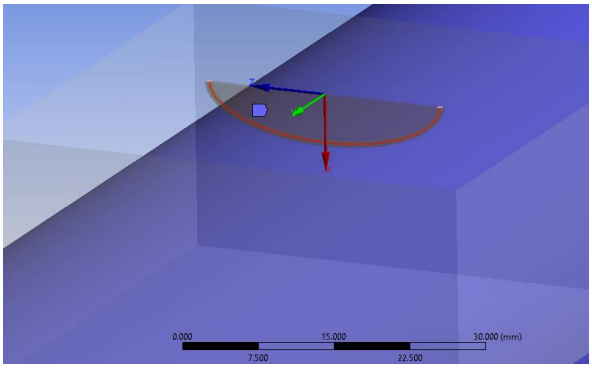

Figure 2: Modelling of crack depth ratio, a/D and crack aspect ratio, a/b

2.3 Crack configuration

The two types of cracks considered in this study are introduced in this section. They are circumferential surface cracks with parallel and non-coplanar parallels. On the surface of the cylinder, two crack morphologies have been examined. The initial coordinate of X and Y axis for the reference crack will be fixed at (0, 25) for α=0 for the parallel configuration, while the coordinates of X and Y axis for the observed crack will vary based on the angle of inclination for the non-coplanar parallel configuration, (6.47, 24.15) for α=15.

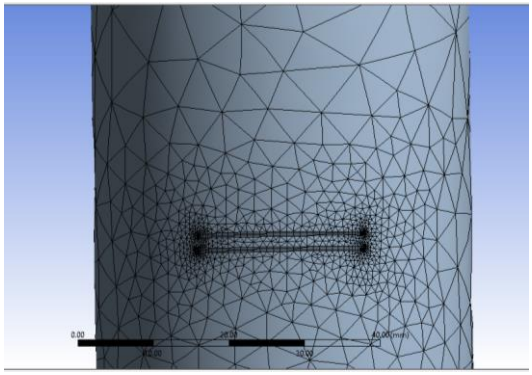

Figure 3: Parallel crack configuration

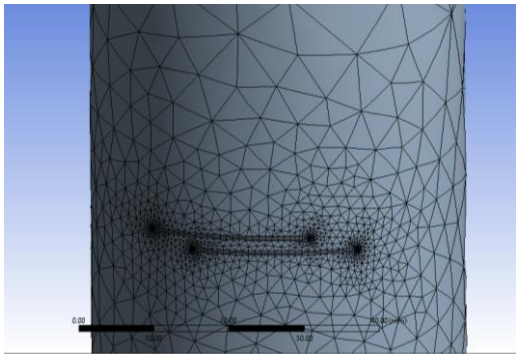

Figure 4: Non-coplanar crack configuration

3. Determination of Interaction Factor

The interaction factor, Ψ is determined depending on SIF in this analysis. Therefore, the SIF must go through three stages in order to calculate the Ψ. SIF is extracted from Ansys in the first step. In the second stage, the SIF extracted is normalized according to the form of loading to ensure the universality of the results. In the third and final stage, Ψ is determined. ANSYS is used in the present study to model and analyse problems regarding multiple cracks

3.1 Normalization of stress intensity factor

Ansys offers the ability to create an infinite number of contours around the tip of the crack. These profiles are numbered radially outwards. The SIF at each contour was calculated in this work, six contours are produced around the crack tip during the analysis process, as shown in Figure 5.

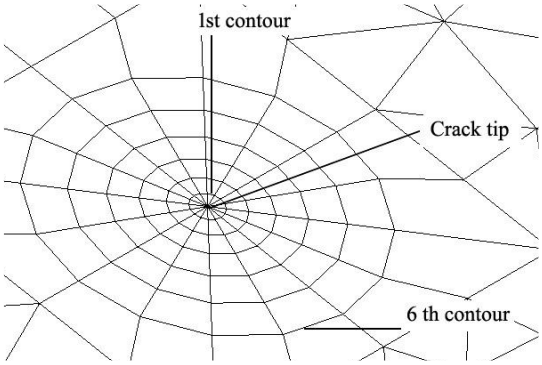

Figure 5: Alignment of contours around crack tip

Based on the literatures, it should be taken note that for each type of loading, a separate equation is used to normalize the SIFs depending on the type and mode of loading. For tension loading, normalized SIF, F can be defined as (AE Ismail, 2012):

$$F_t = \frac{K_t}{\sigma_t \sqrt{\pi a}} \quad (1)$$

Where Ft is the uniform SIF under the tensile load, Kt is the measured SIF under the tensile force (value derived from the sixth contour), σt t is the axial stress, where σt = P/A, P is the applied force, A = area.

For bending load, the normalized SIF, F can be defined as:

$$F_b = \frac{K_b}{\sigma_b \sqrt{\pi a}} \quad (2)$$

Where F_b is the normalized mode I SIF under bending load. K_b is the calculated SIF under bending load. σb is the maximum bending stress, σb = M/I, where M is the moment applied. The SIF under torsional loading are as follows:

$$F_{tor\text{-}II} = \frac{K_{tor-II}}{\tau \max \sqrt{\pi a}} \quad (3)$$

$$F_{tor\text{-}III} = \frac{K_{tor-III}}{\tau \max \sqrt{\pi a}} \quad (4)$$

Where $F_{tor\text{-}II}$ is the normalized SIF for mode II and $F_{tor\text{-}II}$ is the normalized SIF for mode III under torsion load. K_{tor-II} and $K_{tor-III}$ are the calculated SIF for modes II and III respectively, under torsion loading. τmax is the maximum shear stress given by:

$$\tau \max = \frac{T(R)}{J} \quad (5)$$

Where T is the applied torque, R is the radius of the cylinder and J is the polar moment of inertia given by:

$$J = \frac{\pi (D)}{32} \tag{6}$$

Where D is the diameter of the cylinder. In addition, when loading in mixed mode, stress and bending are combined with torsion and applied remotely to the cylinder. Due to this method of loading, the SIF of all three modes is measured, and then each mode is normalized separately. Finally, due to the product of the combined load, the SIF is equal to the F_{EQV}, i.e.:

$$F_{EQV} = \sqrt{(F_I)^2 + (\lambda F_{II})^2 + (\frac{\lambda F_{III}}{1-\nu})^2} \tag{7}$$

Where F_I, F_{II} and F_{III} are the normalized SIFs for each mode respectively under mixed, mode loading. λ is the ratio between shear stress and bending stress.

3.2 Determination of interaction factor

The interaction factor, Ψ is known as the SIF ratio in the case of two cracks to the SIF in the case of a single crack. As an example, Ψ for torsion is the ratio of the normalized SIFs for two cracks to single crack in tension loading. The crack interaction factor can be expressed as:

$$\Psi = \frac{F_{Double\ Crack}}{F_{Single\ Crack}} \tag{8}$$

Where, $F_{Double\ Crack}$ represents the normalized SIF for 2 cracks of any mode and F_{Single} represents the single crack of any mode.

On the other hand, the effect of cracks on SIF can be demonstrated by three forms. The first is to amplify or improve the effect, which shows that the normalized SIF of two cracks is found to be higher than the normalized SIF of a single crack due to crack interaction. The second is the shielding effect in which, due to crack interaction, it is found that the normalized SIF of two cracks is smaller than the normalized SIF of a single crack. The third form is the case where there is no contact between cracks, where each crack can be considered an isolated crack.

Based on the forms mentioned, it is crucial to organise the judgement rules. Therefore, the following formulae are utilised for this purpose:

$$\Psi > 1 + \Psi c \tag{9a}$$

$$\Psi < 1 - \Psi c \tag{9b}$$

therefore,

$$1 - \Psi c > \Psi > 1 + \Psi c \tag{10}$$

4. Results and Discussion

4.1 Interaction analysis for singular and multiple parallel cracks

Tension load was applied on the cylinder to examine the mode I loading. Different types of loadings used causes the cylinder to have different modes of failure. To present the tension mode I of failure, the term Ft was presented which was determined using equation (1).

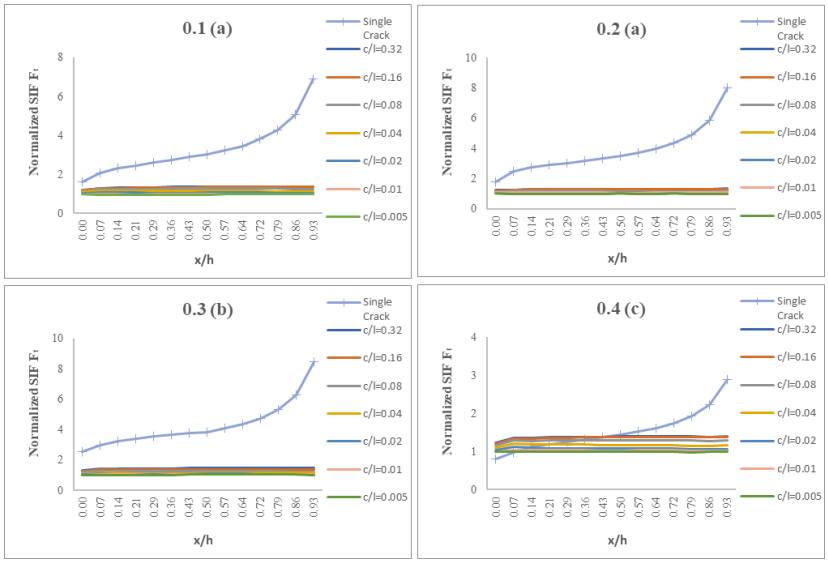

Figure 6: The normalized SIFs for parallel cracks under tension, a/b=0.4 and a/D=0.1 (a), a/D=0.2(b), a/D=0.3(c), a/D=0.4(d)

It should be noted that the Ft distribution pattern is absolutely different, but closer to the single crack trend in the separation distance ratio c/l when the a/D increases. It can be seen from the figure that the higher c/l ratio represents the increase in distance between cracks, and Ft approaches the single crack value, which means that the crack interaction has a greater effect when the cracks are positioned close to each other. As the cracks are positioned away from each other, the lesser the influence of the neighbouring crack.

Table 1: Interaction factor for parallel external cracks under torsion when a/b=0.4

a/b = 0.4 a/D = 0.1 Ψ							
x/h	c/l = 0.005	c/l = 0.01	c/l = 0.02	c/l = 0.04	c/l = 0.08	c/l=0.16	c/l=0.32
0.00	0.49	0.49	0.50	0.50	0.56	0.59	0.59
0.50	0.25	0.26	0.27	0.27	0.33	0.35	0.35
0.93	0.11	0.11	0.12	0.12	0.14	0.15	0.16
a/D = 0.2 Ψ							
x/h	c/l = 0.005	c/l = 0.01	c/l = 0.02	c/l = 0.04	c/l = 0.08	c/l=0.16	c/l=0.32
0.00	0.45	0.47	0.45	0.45	0.51	0.54	0.54
0.50	0.23	0.24	0.23	0.23	0.26	0.29	0.30
0.93	0.10	0.11	0.10	0.10	0.12	0.13	0.13
a/D = 0.3 Ψ							
x/h	c/l = 0.005	c/l = 0.01	c/l = 0.02	c/l = 0.04	c/l = 0.08	c/l=0.16	c/l=0.32
0.00	0.31	0.31	0.32	0.32	0.37	0.39	0.40
0.50	0.21	0.22	0.22	0.22	0.26	0.29	0.30
0.93	0.10	0.10	0.10	0.10	0.11	0.13	0.14
a/D = 0.4 Ψ							
x/h	c/l = 0.005	c/l = 0.01	c/l = 0.02	c/l = 0.04	c/l = 0.08	c/l=0.16	c/l=0.32
0.00	0.31	0.31	0.32	0.32	0.37	0.39	0.40

0.50	0.21	0.22	0.22	0.22	0.26	0.29	0.30
0.93	0.10	0.10	0.10	0.10	0.11	0.13	0.14

Based on the F_t distribution along the crack front. It is crystal clear that maximum interaction occurs at the point, at x/h=0.93. The interaction also can be observed increasing as the values of a/D increase. However, when the distance between cracks increases, represented by c/l, the interactions were reduced. When placed, near to each other, the parallel cracks interact more. Furthermore, the deeper the crack, the larger the separation needed for the crack to be free of the influence of neighbouring crack.

To present the bending mode I of failure, the term Fb was presented which was determined using equation (2). The normalized SIF distribution F_b of parallel external cracks under bending load is shown in Figure 4.2, where the aspect ratio is a/b=0.4, aspect depth ratio of a/D=0.1, 0.2, 0.3 and 0.4. When compared to the tension load in Figure 4.1, the F_b pattern in bending load is almost identical to the parallel crack, but the amplitude is lower. Similarly, the a/D ratio adjustment causes the opposite effect that can be seen under tension load.

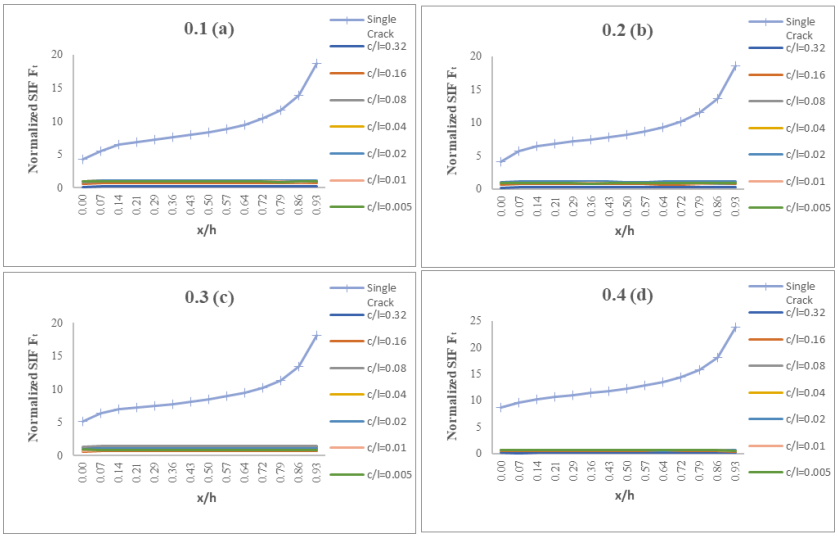

Figure 7: The normalized SIFs for parallel cracks under bending, a/b=0.4 and a/D=0.1 (a), a/D=0.2(b), a/D=0.3(c), a/D=0.4(d)

The interaction factors of two parallel crack configurations under bending load are shown in table 4.2 when a/b = 0.4 and a/t = 0.1, 0.2, 0.3 and 0.4. The outcomes of the interaction factor suggest that point x/h=0.93 has had a serious interaction relative to point x/h=0.5 and 0. This effect is proportional to the increase in crack depth, where a higher interaction effect is seen by high crack depth, and vice versa.

Table 2: Interaction factor for parallel external cracks under bending when a/b=0.4

a/b = 0.4							
a/D = 0.1							
Ψ							
x/h	c/l = 0.005	c/l = 0.01	c/l = 0.02	c/l = 0.04	c/l = 0.08	c/l=0.16	c/l=0.32
0.00	0.22	0.22	0.22	0.22	0.21	0.16	0.05
0.50	0.11	0.11	0.11	0.11	0.11	0.09	0.03
0.93	0.05	0.05	0.05	0.05	0.05	0.04	0.01
a/D = 0.2							
Ψ							

x/h	c/l = 0.005	c/l = 0.01	c/l = 0.02	c/l = 0.04	c/l = 0.08	c/l=0.16	c/l=0.32
0.00	0.22	0.22	0.23	0.23	0.21	0.15	0.05
0.50	0.11	0.11	0.13	0.13	0.10	0.08	0.03
0.93	0.05	0.05	0.06	0.06	0.04	0.04	0.01
a/D = 0.3							
Ψ							
x/h	c/l = 0.005	c/l = 0.01	c/l = 0.02	c/l = 0.04	c/l = 0.08	c/l=0.16	c/l=0.32
0.00	0.17	0.14	0.21	0.21	0.26	0.12	0.24
0.50	0.10	0.10	0.13	0.13	0.17	0.08	0.15
0.93	0.05	0.05	0.06	0.06	0.08	0.04	0.07
a/D = 0.4							
Ψ							
x/h	c/l = 0.005	c/l = 0.01	c/l = 0.02	c/l = 0.04	c/l = 0.08	c/l=0.16	c/l=0.32
0.00	0.08	0.08	0.08	0.08	0.08	0.06	0.02
0.50	0.05	0.05	0.05	0.05	0.05	0.04	0.02
0.93	0.03	0.03	0.03	0.03	0.03	0.02	0.01

Two parallel external cracks were inspected under pure torsional load, of which only F_{tor-II} and $F_{tor-III}$ were measured, indicating the uniform SIF of mode II and III under torsional load. Therefore, there will be no interaction for mode I. The orientation of the normalized SIFs as a function of the normalized crack front position, x/h for mode II and III respectively were shown in figure 8 and 9. Normalized SIF for bending mode II and III were calculated using equations (3) and (4) respectively.

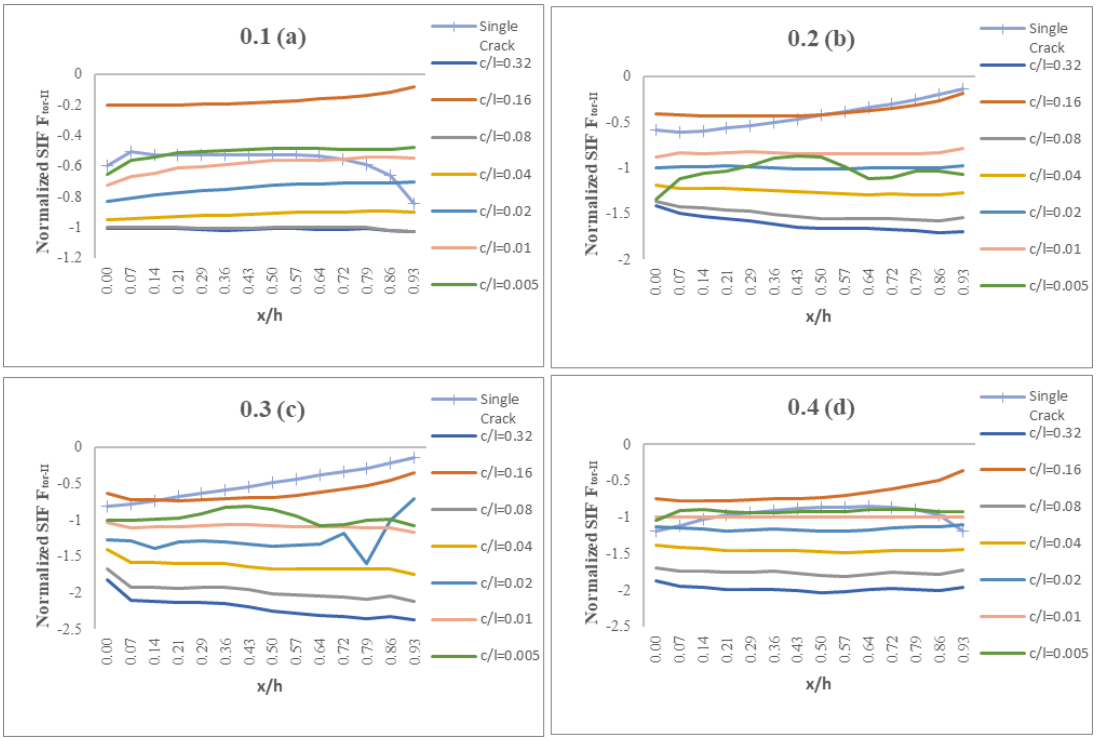

Figure 8: The normalized SIFs for parallel cracks under torsion mode II, a/b=0.4 and a/D=0.1 (a), a/D=0.2(b), a/D=0.3(c), a/D=0.4(d)

Figure 8 displays the trend of F_{tor-II}, when a/b=0.4, for a/D=0.1,0.2,0.3 and 0.4. F_{tor-II} in the case of two cracks for the shallower depth are inversely proportional to the single crack. However, as the a/D goes deeper, especially at at a/D=0.3 and 0.4, the case for two cracks for the depths are mostly

directly proportional to the single crack as the shape of the graphs for two cracks follow the shape of the single crack.

Table 3 indicates the interaction factor, Ψ for the two parallel cracks under torsion with respect to mode II failure. Based on the results of Ψ shown under torsion loading for mode II, the parallel cracks have an interaction with one another. When the crack is at its deepest and shallowest, at a/D=0.1 and 0.4, the cracks have amplification effect, while at a/D=0.2 and 0.3, the cracks lean more to shielding effect.

Table 3: Interaction factor for parallel external cracks under torsion mode II when a/b=0.4

a/b = 0.4							
a/D = 0.1							
Ψ							
x/h	c/l = 0.005	c/l = 0.01	c/l = 0.02	c/l = 0.04	c/l = 0.08	c/l=0.16	c/l=0.32
0.00	2.30	1.51	1.71	1.71	2.33	0.70	2.43
0.50	2.08	1.99	2.39	2.39	3.64	0.98	3.91
0.93	7.97	5.86	7.26	7.26	11.47	1.42	12.56
a/D = 0.2							
Ψ							
x/h	c/l = 0.005	c/l = 0.01	c/l = 0.02	c/l = 0.04	c/l = 0.08	c/l=0.16	c/l=0.32
0.00	0.87	0.83	0.95	0.95	1.42	0.63	1.56
0.50	1.07	1.15	1.37	1.37	2.07	0.84	2.35
0.93	0.78	0.84	0.93	0.93	1.45	0.31	1.65
a/D = 0.3							
Ψ							
x/h	c/l = 0.005	c/l = 0.01	c/l = 0.02	c/l = 0.04	c/l = 0.08	c/l=0.16	c/l=0.32
0.00	1.10	1.21	1.40	1.40	1.68	0.34	1.69
0.50	0.93	1.08	1.38	1.38	1.91	0.35	1.92
0.93	0.57	0.65	0.83	0.83	1.22	0.10	1.22
a/D = 0.4							
Ψ							
x/h	c/l = 0.005	c/l = 0.01	c/l = 0.02	c/l = 0.04	c/l = 0.08	c/l=0.16	c/l=0.32
0.00	1.23	1.27	1.56	1.56	2.06	0.77	2.23
0.50	1.73	2.21	2.76	2.76	4.10	1.41	4.59
0.93	7.23	7.78	4.72	4.72	14.16	2.36	15.89

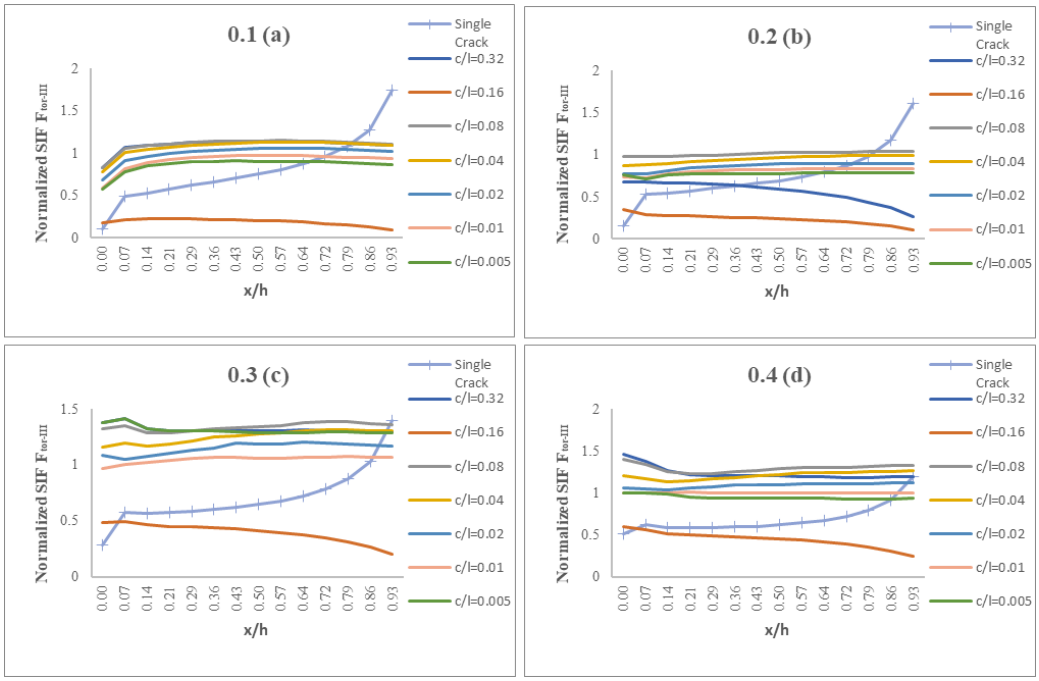

Figure 9: The normalized SIFs for parallel cracks under torsion mode III, a/b=0.4 and a/D=0.1 (a), a/D=0.2(b), a/D=0.3(c), a/D=0.4(d)

Figure 9 shows the distribution of normalized SIFs for mode III under torsion loading for parallel cracks, $F_{tor\text{-}III}$. As shown by the graph, $F_{tor\text{-}III}$ distributed along the crack front where the maximum value was achieved at the deepest point of the crack at a/D=0.2 onwards. The single crack was not much affected by the change of the depth of the crack, a/D. this means that under torsion loading, the effect of changes in crack depth for $F_{tor\text{-}III}$ was not significant.

Table 4: Interaction factor for parallel external cracks under torsion mode III when a/b=0.4

a/b = 0.4							
a/D = 0.1							
Ψ							
x/h	c/l = 0.005	c/l = 0.01	c/l = 0.02	c/l = 0.04	c/l = 0.08	c/l=0.16	c/l=0.32
0.00	3.34	1.68	1.86	1.86	2.17	0.44	2.18
0.50	2.87	1.30	1.41	1.41	1.53	0.27	1.51
0.93	2.55	0.53	0.59	0.59	0.63	0.05	0.62
a/D = 0.2							
Ψ							
x/h	c/l = 0.005	c/l = 0.01	c/l = 0.02	c/l = 0.04	c/l = 0.08	c/l=0.16	c/l=0.32
0.00	2.77	1.89	2.02	2.02	2.55	0.75	2.62
0.50	2.34	1.48	1.60	1.60	1.83	0.46	1.81
0.93	2.13	0.61	0.67	0.67	0.77	0.09	0.75
a/D = 0.3							
Ψ							
x/h	c/l = 0.005	c/l = 0.01	c/l = 0.02	c/l = 0.04	c/l = 0.08	c/l=0.16	c/l=0.32
0.00	2.11	1.74	1.82	1.82	2.34	0.86	2.44
0.50	2.04	1.64	1.84	1.84	2.08	0.64	2.02
0.93	1.99	0.76	0.84	0.84	0.97	0.14	0.93
a/D = 0.4							
Ψ							

x/h	c/l = 0.005	c/l = 0.01	c/l = 0.02	c/l = 0.04	c/l = 0.08	c/l=0.16	c/l=0.32
0.00	1.68	1.59	1.66	1.66	2.13	0.90	2.20
0.50	1.76	1.61	1.78	1.78	2.08	0.73	1.94
0.93	1.74	0.84	0.94	0.94	1.11	0.20	1.00

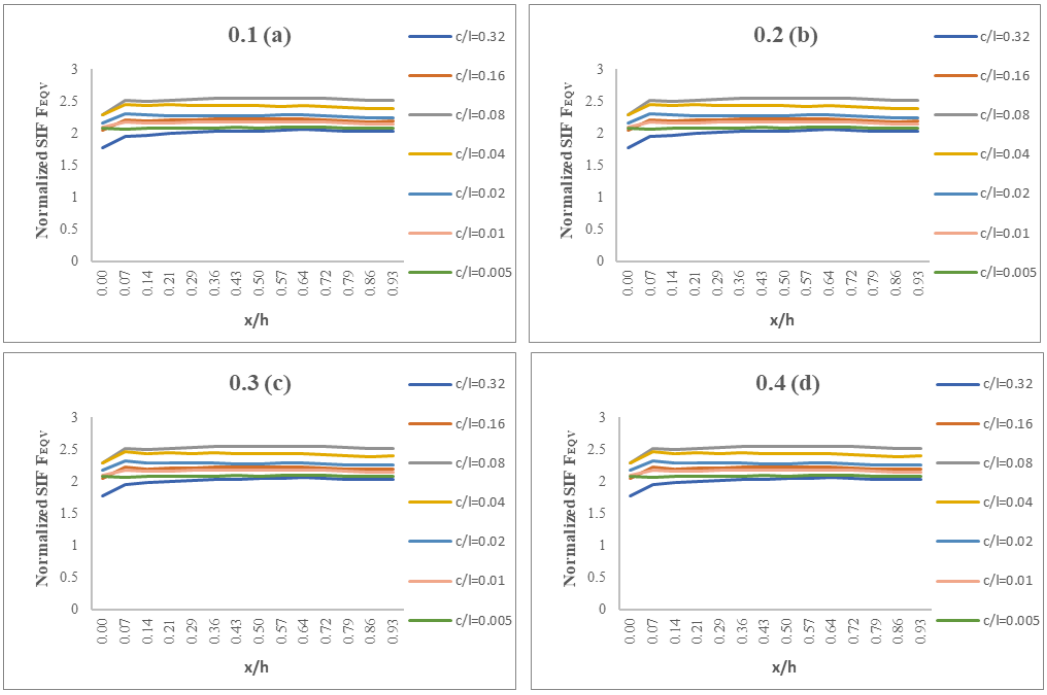

Figure 10: The normalized SIFs for parallel cracks under mixed-mode, a/b=0.4 and a/D=0.1 (a), a/D=0.2(b), a/D=0.3(c), a/D=0.4(d)

Table 5: Interaction factor for parallel external cracks under mixed-mode when a/b=0.4

a/b = 0.4

a/D = 0.1

Ψ

x/h	c/l = 0.005	c/l = 0.01	c/l = 0.02	c/l = 0.04	c/l = 0.08	c/l=0.16	c/l=0.32
0.93	0.70	0.70	0.73	0.77	0.76	0.69	0.59
0.50	0.36	0.36	0.40	0.42	0.44	0.39	0.36
0.00	0.16	0.16	0.17	0.19	0.20	0.17	0.16

a/D = 0.2

Ψ

x/h	c/l = 0.005	c/l = 0.01	c/l = 0.02	c/l = 0.04	c/l = 0.08	c/l=0.16	c/l=0.32
0.93	0.75	0.75	0.74	0.75	0.80	0.69	0.62
0.50	0.35	0.35	0.39	0.39	0.41	0.34	0.34
0.00	0.16	0.16	0.17	0.17	0.18	0.15	0.15

a/D = 0.3

Ψ

x/h	c/l = 0.005	c/l = 0.01	c/l = 0.02	c/l = 0.04	c/l = 0.08	c/l=0.16	c/l=0.32
0.93	0.62	0.62	0.64	0.63	0.78	0.67	0.79
0.50	0.37	0.37	0.43	0.42	0.53	0.45	0.54
0.00	0.17	0.17	0.19	0.19	0.24	0.20	0.26

a/D = 0.4

Ψ

x/h	c/l = 0.005	c/l = 0.01	c/l = 0.02	c/l = 0.04	c/l = 0.08	c/l=0.16	c/l=0.32
0.93	0.42	0.42	0.44	0.48	0.53	0.42	0.48
0.50	0.28	0.28	0.31	0.34	0.37	0.29	0.34
0.00	0.14	0.14	0.16	0.18	0.19	0.14	0.17

The trend of $F_{EQV-EXT}$ was illustrated in figure 4-5 when a/b=0.2, a/D =0.1, 0.2, 0.3, 0.4. From the graph, we can observe that while having the same aspect ratio, a/b, the change in $F_{EQV-EXT}$ can be observed when the crack depth ratio changes. The value of x/h has a direct proportion relationship with a/D. A higher value of a/D resulted in a slight convex-curved shape while a lower value of a/D resulted in a more concave-curved shape.

4.2 Interaction analysis for singular and multiple non-coplanar parallel cracks

As previously mentioned, the non-coplanar parallel crack configuration for the cylinder was analysed under different types of loadings, similar to parallel cracks. For the cylinder, the considered angle of inclination of the cracks was α=15°.

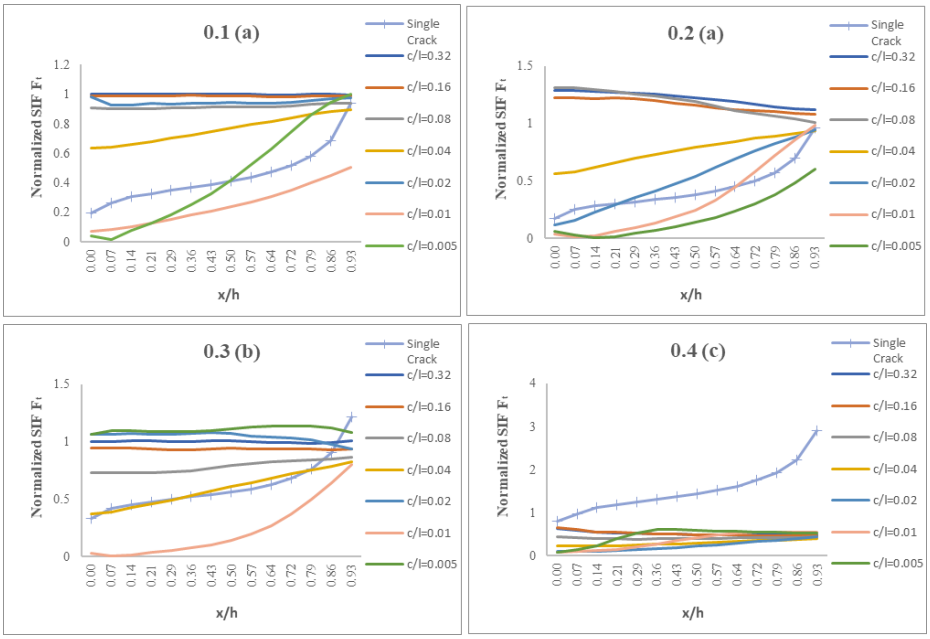

Figure 11: The normalized SIFs for parallel cracks under tension, a/b=0.4 and a/D=0.1 (a), a/D=0.2(b), a/D=0.3(c), a/D=0.4(d), α=15°

The distribution of Ft for two cracks for c/l=0.005 and 0.01 shows shielding effect for every a/D, except for an a/D=0.3 where the cracks exhibit amplification effect at x/h=0 & 0.5. Cracks in a/D=0.4 all having shielding effect. This proves that the deeper the cracks are, the more the neighbouring cracks have less impact until the depth reaches a/D=0.4.

Table 6: Interaction factor for parallel external cracks under tension when a/b=0.4, α=15°

a/b = 0.4							
a/D = 0.1							
Ψ							
x/h	c/l = 0.005	c/l = 0.01	c/l = 0.02	c/l = 0.04	c/l = 0.08	c/l=0.16	c/l=0.32
0.00	0.21	0.35	5.00	5.00	4.60	5.04	5.09
0.50	1.02	0.58	2.30	2.30	2.23	2.41	2.44
0.93	1.07	0.54	1.04	1.04	1.00	1.06	1.06
a/D = 0.2							

Ψ

x/h	c/l = 0.005	c/l = 0.01	c/l = 0.02	c/l = 0.04	c/l = 0.08	c/l=0.16	c/l=0.32
0.00	0.33	0.21	0.70	0.70	7.67	7.14	7.50
0.50	0.36	0.64	1.43	1.43	3.15	3.06	3.22
0.93	0.63	1.03	0.98	0.98	1.05	1.12	1.16

a/D = 0.3

Ψ

x/h	c/l = 0.005	c/l = 0.01	c/l = 0.02	c/l = 0.04	c/l = 0.08	c/l=0.16	c/l=0.32
0.00	3.23	0.08	3.24	3.24	2.23	2.88	3.05
0.50	1.99	0.26	1.92	1.92	1.42	1.68	1.80
0.93	0.88	0.66	0.77	0.77	0.71	0.77	0.83

a/D = 0.4

Ψ

x/h	c/l = 0.005	c/l = 0.01	c/l = 0.02	c/l = 0.04	c/l = 0.08	c/l=0.16	c/l=0.32
0.00	0.11	0.11	0.11	0.28	0.56	0.82	0.79
0.50	0.41	0.30	0.15	0.20	0.27	0.34	0.36
0.93	0.18	0.19	0.15	0.14	0.15	0.16	0.16

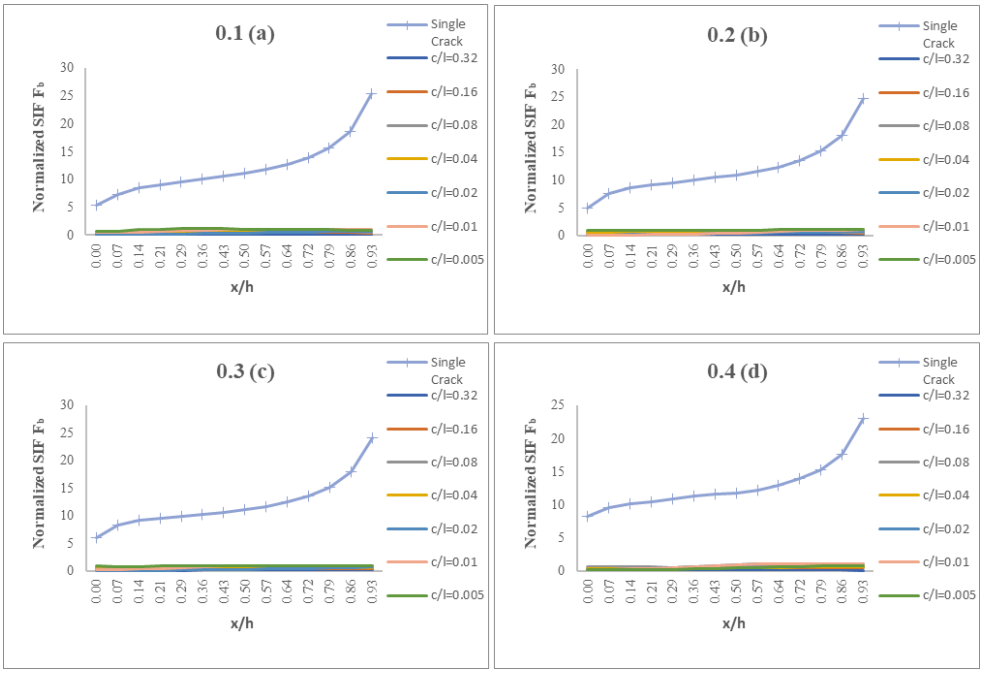

Figure 12: The normalized SIFs for parallel cracks under bending, a/b=0.4 and a/D=0.1 (a), a/D=0.2(b), a/D=0.3(c), a/D=0.4(d), α=15^{O}

At α=15^{o}, the graph exhibits the similar shape to the parallel configuration when subjected to bending, Fb. The amplitude of the graph is much lower than that of the parallel crack configuration. the interaction factor, Ψ for non-coplanar cracks under bending load. The interaction between cracks were further impacted as the value of c/l increases. This indicates that the further away the cracks are from each other, the more the interaction between neighbouring cracks.

Table 7: Interaction factor for parallel external cracks under bending when a/b=0.4, α=15^{O}

a/b = 0.4							
a/D = 0.1							
Ψ							
x/h	c/l = 0.005	c/l = 0.01	c/l = 0.02	c/l = 0.04	c/l = 0.08	c/l=0.16	c/l=0.32
0.00	0.22	0.22	0.22	0.22	0.21	0.16	0.05
0.50	0.11	0.11	0.11	0.11	0.11	0.09	0.03
0.93	0.05	0.05	0.05	0.05	0.05	0.04	0.01
a/D = 0.2							
Ψ							
x/h	c/l = 0.005	c/l = 0.01	c/l = 0.02	c/l = 0.04	c/l = 0.08	c/l=0.16	c/l=0.32
0.00	0.22	0.22	0.23	0.23	0.21	0.15	0.05
0.50	0.11	0.11	0.13	0.13	0.10	0.08	0.03
0.93	0.05	0.05	0.06	0.06	0.04	0.04	0.01
a/D = 0.3							
Ψ							
x/h	c/l = 0.005	c/l = 0.01	c/l = 0.02	c/l = 0.04	c/l = 0.08	c/l=0.16	c/l=0.32
0.00	0.17	0.14	0.21	0.21	0.26	0.12	0.24
0.50	0.10	0.10	0.13	0.13	0.17	0.08	0.15
0.93	0.05	0.05	0.06	0.06	0.08	0.04	0.07
a/D = 0.4							
Ψ							
x/h	c/l = 0.005	c/l = 0.01	c/l = 0.02	c/l = 0.04	c/l = 0.08	c/l=0.16	c/l=0.32
0.00	0.08	0.08	0.08	0.08	0.08	0.06	0.02
0.50	0.05	0.05	0.05	0.05	0.05	0.04	0.02
0.93	0.03	0.03	0.03	0.03	0.03	0.02	0.01

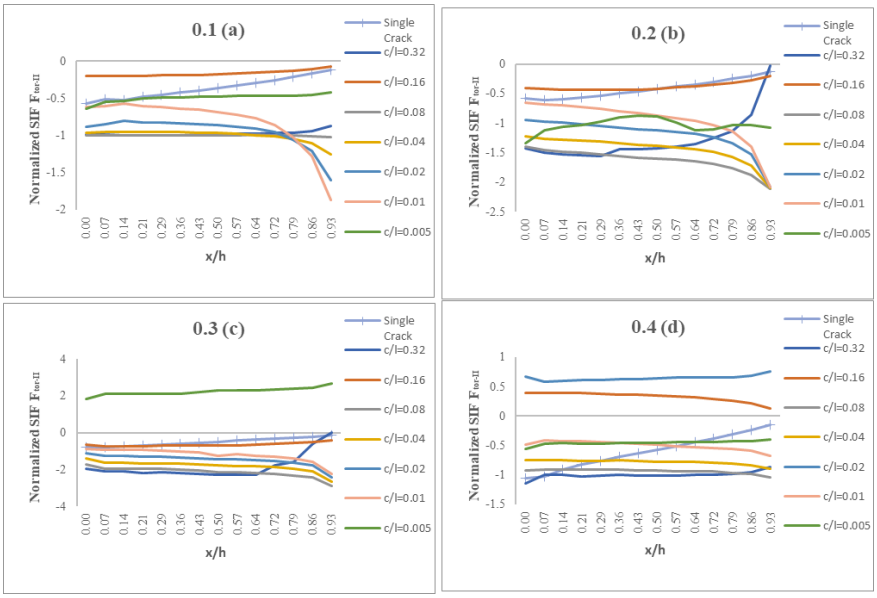

Figure 13: The normalized SIFs for parallel cracks under torsion mode II, a/b=0.4 and a/D=0.1 (a), a/D=0.2(b), a/D=0.3(c), a/D=0.4(d), α=15^{O}

The F_{tor-II} exhibited mostly an opening mode. It also shows amplifying effect at x/h=0 for all points except at a/D=0.4. The interaction between cracks were more significant at a/D=0.1 and a/D=0.4. Most of the cracks at a/D=0.1 and 0.4 were showing the effects of shielding at point x/h=0.93. At a/D=0.2 and 0.3 however, the opposite happens where at x/h=0.93 show amplification effects.

Table 8: Interaction factor for parallel external cracks under torsion mode II when a/b=0.4, α=15^{O}

a/b = 0.4							
a/D = 0.1							
Ψ							
x/h	c/l = 0.005	c/l = 0.01	c/l = 0.02	c/l = 0.04	c/l = 0.08	c/l=0.16	c/l=0.32
0.00	1.10	1.21	1.40	1.40	1.68	0.34	1.69
0.50	0.93	1.08	1.38	1.38	1.91	0.35	1.92
0.93	0.57	0.65	0.83	0.83	1.22	0.10	1.22
a/D = 0.2							
Ψ							
x/h	c/l = 0.005	c/l = 0.01	c/l = 0.02	c/l = 0.04	c/l = 0.08	c/l=0.16	c/l=0.32
0.00	2.30	1.51	1.71	1.71	2.33	0.70	2.43
0.50	2.08	1.99	2.39	2.39	3.64	0.98	3.91
0.93	7.97	5.86	7.26	7.26	11.47	1.42	12.56
a/D = 0.3							
Ψ							
x/h	c/l = 0.005	c/l = 0.01	c/l = 0.02	c/l = 0.04	c/l = 0.08	c/l=0.16	c/l=0.32
0.00	1.23	1.27	1.56	1.56	2.06	0.77	2.23
0.50	1.73	2.21	2.76	2.76	4.10	1.41	4.59
0.93	7.23	7.78	4.72	4.72	14.16	2.36	15.89
a/D = 0.4							
Ψ							
x/h	c/l = 0.005	c/l = 0.01	c/l = 0.02	c/l = 0.04	c/l = 0.08	c/l=0.16	c/l=0.32
0.00	0.87	0.83	0.95	0.95	1.42	0.63	1.56
0.50	1.07	1.15	1.37	1.37	2.07	0.84	2.35
0.93	0.78	0.84	0.93	0.93	1.45	0.31	1.65

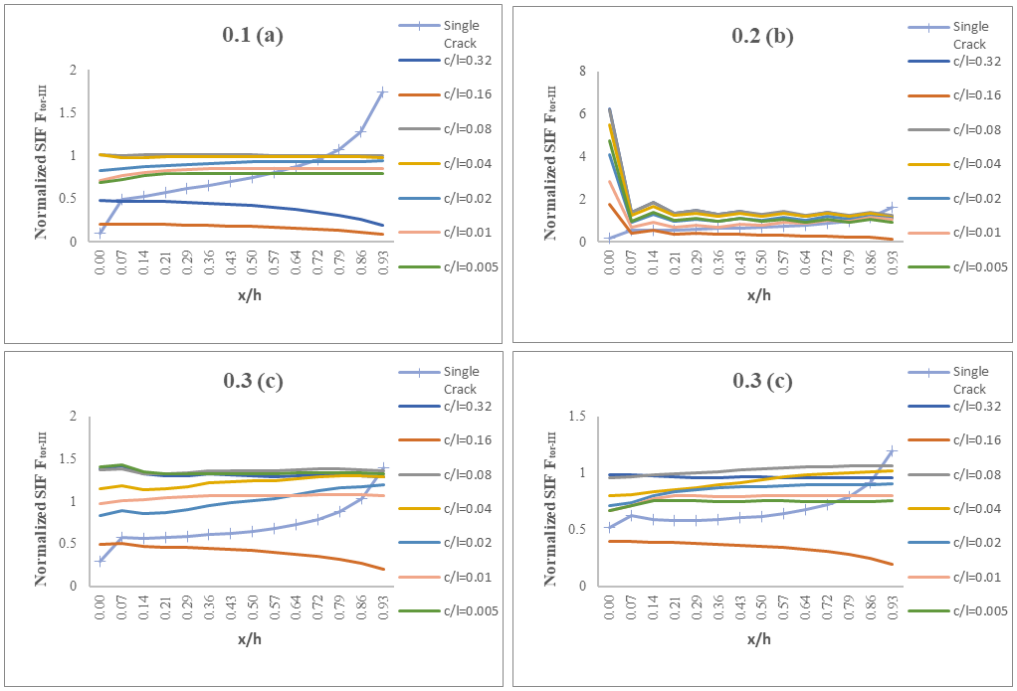

Figure 14: The normalized SIFs for parallel cracks under torsion mode III, a/b=0.4 and a/D=0.1 (a), a/D=0.2(b), a/D=0.3(c), a/D=0.4(d), $\alpha=15^{O}$

The $F_{tor\text{-}III}$ shows amplifying effect at for all points of a/D, except at c/l=0.16, where the cracks exhibit shielding effect. The interaction between cracks were more significant as the a/D increase. This indicates that as the distance between cracks increase, the larger the effect of the neighbouring crack impacting the targeted crack.

Table 9: Interaction factor for parallel external cracks under torsion mode III when a/b=0.4, $\alpha=15^{O}$

a/b = 0.4							
a/D = 0.1							
Ψ							
x/h	c/l = 0.005	c/l = 0.01	c/l = 0.02	c/l = 0.04	c/l = 0.08	c/l=0.16	c/l=0.32
0.00	3.34	1.68	1.86	1.86	2.17	0.44	2.18
0.50	2.87	1.30	1.41	1.41	1.53	0.27	1.51
0.93	2.55	0.53	0.59	0.59	0.63	0.05	0.62
a/D = 0.2							
Ψ							
x/h	c/l = 0.005	c/l = 0.01	c/l = 0.02	c/l = 0.04	c/l = 0.08	c/l=0.16	c/l=0.32
0.00	2.77	1.89	2.02	2.02	2.55	0.75	2.62
0.50	2.34	1.48	1.60	1.60	1.83	0.46	1.81
0.93	2.13	0.61	0.67	0.67	0.77	0.09	0.75
a/D = 0.3							
Ψ							
x/h	c/l = 0.005	c/l = 0.01	c/l = 0.02	c/l = 0.04	c/l = 0.08	c/l=0.16	c/l=0.32
0.00	2.11	1.74	1.82	1.82	2.34	0.86	2.44
0.50	2.04	1.64	1.84	1.84	2.08	0.64	2.02
0.93	1.99	0.76	0.84	0.84	0.97	0.14	0.93
a/D = 0.4							
Ψ							

x/h	c/l = 0.005	c/l = 0.01	c/l = 0.02	c/l = 0.04	c/l = 0.08	c/l=0.16	c/l=0.32
0.00	1.68	1.59	1.66	1.66	2.13	0.90	2.20
0.50	1.76	1.61	1.78	1.78	2.08	0.73	1.94
0.93	1.74	0.84	0.94	0.94	1.11	0.20	1.00

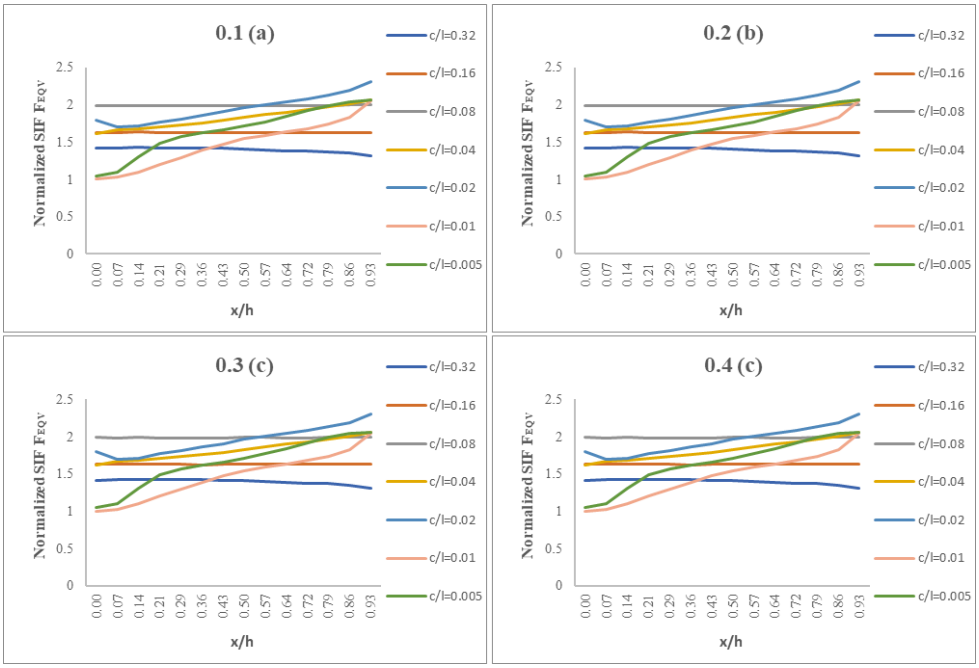

Figure 15: The normalized SIFs for parallel cracks under torsion mixed-mode, a/b=0.4 and a/D=0.1 (a), a/D=0.2(b), a/D=0.3(c), a/D=0.4(d), $\alpha=15^{O}$

F_{EQV} shows a concave pattern for all a/D. Lower crack depth values, a/D=0.005, 0.01, 0.02 and 0.04 shows an increase graph while the values of higher crack depth ratio, a/D=0.08, 0.16 and 0.32 have decreasing values. The interaction of cracks is more visible as the value of x/h increase. All of the cracks show shielding effect, except at point x/h=0 at a/D=0.2.

Table 10: Interaction factor for parallel external cracks under mixed-mode when a/b=0.4, $\alpha=15^{O}$

a/b = 0.4							
a/D = 0.1							
Ψ							
x/h	c/l = 0.005	c/l = 0.01	c/l = 0.02	c/l = 0.04	c/l = 0.08	c/l=0.16	c/l=0.32
0.00	0.38	0.38	0.65	0.58	0.71	0.59	0.51
0.50	0.29	0.29	0.34	0.31	0.34	0.28	0.24
0.93	0.16	0.16	0.17	0.16	0.15	0.12	0.10
a/D = 0.2							
Ψ							
x/h	c/l = 0.005	c/l = 0.01	c/l = 0.02	c/l = 0.04	c/l = 0.08	c/l=0.16	c/l=0.32
0.00	1.83	1.83	1.54	2.11	2.44	1.01	2.40
0.50	0.27	0.27	0.26	0.37	0.42	0.32	0.36
0.93	0.16	0.16	0.19	0.20	0.19	0.13	0.13
a/D = 0.3							
Ψ							
x/h	c/l = 0.005	c/l = 0.01	c/l = 0.02	c/l = 0.04	c/l = 0.08	c/l=0.16	c/l=0.32
0.00	0.81	0.81	0.48	0.49	0.67	0.45	0.69

0.50	0.48	0.48	0.33	0.34	0.40	0.26	0.39
0.93	0.23	0.23	0.20	0.20	0.21	0.12	0.14

a/D = 0.4

Ψ

x/h	c/l = 0.005	c/l = 0.01	c/l = 0.02	c/l = 0.04	c/l = 0.08	c/l=0.16	c/l=0.32
0.00	0.17	0.17	0.18	0.23	0.33	0.25	0.32
0.50	0.19	0.19	0.23	0.19	0.23	0.16	0.20
0.93	0.12	0.12	0.14	0.12	0.12	0.08	0.10

5. Conclusion

The finite element analysis to determine the SIFs for semi elliptical parallel surface cracks has been conducted on a solid cylinder. There were various range of crack geometrical parameters such as crack depth ratio and crack aspect ratio, as well as crack separation ratio that ranges from close distance to long distance. The SIFs results for the parallel cracks configuration were obtained first. The result from the SIFs were normalized for generalisation to determine the interaction factor to outline the relationship between two cracks and single crack. The results of the tension, bending, torsion and mixed-mode SIFs were obtained and then normalized to generalize the results presented in the graphs. However, the findings were contradictory and the graphs obtained were not of the same pattern as the previous studies. Almost all the findings have shown that the double cracks are inversely proportional to the single crack. For torsion and bending loads, double cracks appear to have a similar pattern to a single crack as the ratio of crack distance increases. However, in the case of torsion, the results were random, especially in the crack depth ratio of a/D=0.3 in Mode II and III. In comparison to previous research, cracks appear to interact more in the outermost area than at the deepest point of the crack. In addition, much of the shielding effects often occur in the outermost regions due to cracks instead of the deepest point. For non-coplanar configuration, the tension and bending graphs were identical to the parallel configuration. In the case of torsional load, the graph pattern is becoming increasingly inconsistent, particularly in mode III. Thus, the relationship between parallel crack and non-coplanar torsional configuration cannot be defined.

Acknowledgement

The authors would also like to thank the Faculty of Mechanical and Manufacturing Engineering, Universiti Tun Hussein Onn Malaysia for its support.

References

[1] Nanda, J., Das, S., & Parhi, D. R., “Effect of Slenderness Ratio on Crack Parameters of Simply Supported Shaft”, *Procedia Materials Science*, *6* (Icmpc), pp. 1428–1435, 2015.

[2] Hellan, Kore, and H. Saunders. “Introduction to Fracture Mechanics.” Journal of Vibration and Acoustics, vol. 109, no. 3, 1987, pp. 325–26.

[3] Griffits, A. A., “ The phenomena of rupture and flow in solids. Masinovedenie”, C (1), pp. 9–14, 1995.

[4] Irwin, G.R., "Fracture Dynamics," Fracturing of Metals, American Society for Metals, Cleveland, OH, pp. 147-166, 1948.

[5] G. R. Irwin, "Analysis of stresses and strains near the end of a crack traversing a plate". J. Applied Mechanics, 24, (1957) pp. 361–364. (n.d.).

[6] Wells, A., "George Rankin Irwin. 26 February 1907-9 October 1998, iographical Memoirs of Fellows of the Royal Society", 46, pp. 271-283, 2000.

[7] Suresh, S., "Plastic Fracture Mechanics" *Fracture Mechanics*, pp. 147–172, 2006.

[8] Zehnder A.T., Griffith, "Theory of Fracture", Encyclopedia of Tribology. Springer, Boston, MA, 2013.

[9] Rice, J. R. "A Path Independent Integral and the Approximate Analysis of Strain Concentration by Notches and Cracks." Journal of Applied Mechanics, vol. 35, no. 2, 1968, pp. 379–86.

[10] Kane, S. N., Mishra, A., & Dutta, A. K., " Preface: International Conference on Recent Trends in Physics (ICRTP 2016)`. *Journal of Physics: Conference Series*, *755*(1), 2016.

[11] Shih, Y. S., & Chen, J. J., 'The stress intensity factor study of an elliptical cracked shaft", *Nuclear Engineering and Design*, *214*(1–2), pp. 137–145, 2002.

[12] Ismail, A. E., Ariffin, A. K., Abdullah, S., Ghazali, M. J., Abdulrazzaq, M., & Daud, R., "Stress intensity factors under combined bending and torsion moments", *Journal of Zhejiang University: Science A*, *13*(1), pp. 1–8, 2012.

[13] MK Awang, AE Ismail, AL Mohd Tobi1 and MH Zainulabidin, "Stress intensity factors and interaction of two parallel surface cracks on cylinder under tension" IOP Conference Series: Materials Science and Engineering, Volume 165, Colloquium of Advanced Mechanics. *Colloquium of Advanced Mechanics (CAMS2016) 18–19 December 2016, Johor, Malaysia*

[14] Ismail, A. E., Jamian, S., Kamarudin, K. A., Mohd Nor, M. K., Ibrahim, M. N., & Choiron, M. A., "An overview of fracture mechanics with ANSYS", *International Journal of Integrated Engineering*, *10*(5), pp. 59–67, 2018.

[15] Anis, S. F., Koyama, M., Hamada, S., & Noguchi, H., "Simplified stress field determination for an inclined crack and interaction between two cracks under tension." *Theoretical and Applied Fracture Mechanics*, *107*(October 2019), 102561, 2020.

[16] Factor, I., "chapter-elastic-stress-around-crack-tip-Elsevier-2012, pp. 25–75, 2012.,

[17] Nanda, J., & Parhi, D. R., " Theoretical analysis of the shaft. *Advances in Fuzzy Systems*, *2013*.

[18] modes123 @ www.fracturemechanics.org. (n.d.). Retrieved from https://www.fracturemechanics.org/modes123.html

[19] fm_intro @ www.efunda.com. (n.d.). Retrieved from https://www.efunda.com/formulae/solid_mechanics/fracture_mechanics/fm_intro.cfm